# Parking search in the physical world: Calculating the search time by leveraging physical and graph theoretical methods

Nilankur Dutta, Thibault Charlottin, Alexandre Nicolas

# Parking search in the physical world: Calculating the search time by leveraging physical and graph theoretical methods

Nilankur DUTTA[a], Thibault CHARLOTTIN[a,b], Alexandre NICOLAS[a]

[a] *Institut Lumière Matière, CNRS and Université Claude Bernard Lyon 1, F-69622 Villeurbanne, France*

[b] *École nationale des travaux publics de l'État (ENTPE), Université de Lyon, F-69518 Vaulx-en-Velin, France*

**Abstract**

Parking plays a central role in transport policies and has wide-ranging consequences: While the average time spent searching for parking exceeds dozens of hours per driver every year in many Western cities, the associated cruising traffic generates major externalities. However, the laws governing the parking search time remain opaque in many regards, which hinders any general understanding of the problem and its determinants. Here, we frame the parking problem in a mathematically well posed manner which puts the focus on the role of the street network and the unequal attractiveness of parking spaces. This problem is solved in two independent ways, valid in any street network and for arbitrary behaviours of the drivers. Numerically, this is done by means of a computationally efficient and versatile agent-based model. Analytically, we leverage the machinery of Statistical Physics and Graph Theory to derive a generic mean-field relation giving the parking search time as a function of the occupancy of parking spaces; an expression for the latter is obtained in the stationary regime. We show that these theoretical results are applicable in toy networks as well as in the complex, large-scale case of the city of Lyon, France. Taken as a whole, these findings clarify the factors that directly control the search time and establish formal connections between the parking issue in realistic settings and physical problems.

*Keywords:* on-street parking, parking search time, street network, graph theory

## 1. Introduction

While cars are inherently designed to move, whether or not to use this mode of transportation is oftentimes less a matter of *driving to* a certain destination than being able to *park* there. Indeed, in many large metropolitan areas, it is hard to overstate the importance of parking on mobility choices and, more broadly, daily life in a city (Shoup, 2018): The time spent

*Email addresses:* nilankur.dutta@gmail.com (Nilankur DUTTA), alexandre.nicolas@polytechnique.edu (Alexandre NICOLAS)

searching for parking exceeds dozens of hours per driver every year (35h to 107h in Western metropolises, according to INRIX survey data (Cookson and Pishue, 2017)), at an estimated cost of several hundred Euros a year per driver. Furthermore, trips that motorists eventually give up because of the lack of parking space are far from being unheard of [1]. Beyond these individual quandaries, cars cruising for parking may represent more than 10% of the total traffic in many large cities (e.g., 15% in central Stuttgart, 28% to 45% in New York), according to surveys and observations of the number of cars driving by a vacant spot before it is occupied (Shoup, 2018; Hampshire and Shoup, 2018), and thus significantly contribute to congestion and pollution in city centres. Admittedly, these quantitative figures are vividly debated and may overestimate the typical share of traffic due to cruising for parking by investigating only the most problematic areas (Weinberger et al., 2020).

Still, there is a broad consensus about the centrality of parking in transport policies. While some cities require developers to add a parking facility to their development plans, through so called minimum parking requirements (Shoup, 2018, chap. 3), in others restrictive parking policies have become an essential lever of action for transport authorities (Boujnah, 2017; Polak and Axhausen, 1990) to curb down the use of private cars. Besides, smart cities are on the rise and intend to alleviate the pains of parking thanks to dynamic parking information and the possibility to book a parking spot, as well as parking guidance systems (Al-Turjman and Malekloo, 2019).

These points call for more reliable observations of the current state of parking in different contexts, but also for a deeper understanding of the process of parking search, so as to be able to predict the impact of hypothetical measures. However, for all its importance, the topic of parking is still fairly opaque, with a limited current grasp of its main factors and their impact. This dim understanding is not surprising given the complexity of the problem, which mingles socio-psychological and economic factors with physical constraints and collective effects. Worse still, it is interwoven with other facets of traffic, such as the local urban traffic. Even some seemingly natural assumptions regarding the relation between occupancy and parking search time (Axhausen et al., 1994; Arnott and Williams, 2017) seem hard to reconcile with facts, albeit commonly used (Geroliminis, 2015).

In this paper, the parking problem is framed in a mathematically well posed manner which puts the focus on the role of the street network and the unequal attractiveness of parking spaces (due to their location and rates, for instance) among other blind spots of existing approaches (Section 2), while leaving aside at present some more studied effects, notably the underlying urban traffic and the elasticity of parking demand. Interesting parallels with problems in the realm of Physics (Schadschneider et al., 2010), more precisely the asymmetric motion of active particles on a graph, then become apparent and clarify some facets of parking search. Importantly, once thus formulated, the parking problem can be solved not only by means of a computationally efficient agent-based algorithm that we developed, but also by leveraging the powerful machinery of Statistical Physics and Graph Theory (Section 3). This

[1] A 2005 survey conducted in 3 French cities indicated that the percentage of interviewees who had at least once given up a trip ('balking') because of parking unavailability amounted to 48% in Grenoble, 67% in Lyon, and 100% in Paris (SARECO / Prédit-Ademe, 2005).

leads to analytical formulae for the search time and for the steady-state occupancy which are valid in remarkably generic settings, for any street network and for a wide range of driving strategies and parking choices. These theoretical results are found to be applicable in toy networks as well as in the complex, large-scale case of the city of Lyon, France (Section 4) and pave the way for theoretical assessments of e.g. the efficiency of smart parking solutions.

## 2. Blind spots of existing approaches to parking search

### *2.1. Literature survey of the determinants of parking search behaviour*

The behaviours and strategies of drivers in search of parking have been examined by means of field observations ('revealed preferences'), surveys ('stated preferences'), and more recently serious games (Fulman et al., 2020). When it comes to the factors that influence parking behaviour, pricing has been intensely studied and plays a major role in parking choice (Shoup, 2018; Gao et al., 2021), which has prompted dynamic pricing strategies to control the occupancy (Chatman and Manville, 2014). The price elasticity of parking volume (i.e., the number of cars that parked in a given duration) generally lies in the range $[-2, -0.2]$, but strongly depends on the context, in particular the average occupancy and the existence of substitutes in terms of parking facilities or mode of transportation (transit service); it is also found to be sensitive to the methodology used, with disagreements between stated and revealed preferences (see (Lehner and Peer, 2019) for a recent meta-analysis). The location of the parking space, and most prominently the distance to destination, is of course another key determinant, both for parking on the curb and for off-street parking, with a strong preference for spots near the ticket machine (if there is one) in parking lots (Vo et al., 2016) or near the facility in rest areas on expressways (Tanaka et al., 2017). This list of *endogenous* features of the parking supply should be completed by mentioning the size of the parking space, the availability of boards with parking guidance information, which may have an influence or not depending on the conditions (Axhausen et al., 1994; Tanaka et al., 2017), etc. All these factors (which are to be subsumed into an 'attractiveness' variable in the following) thus influence the parking search process.

But parking search, in turn, can also affect the driver's decision, with a marked reluctance for long travel times, especially in congested conditions (Gao et al., 2021), and queues (Tanaka et al., 2017). The typical driver thus first drives to the vicinity of the destination (85% of times in the serious game of (Fulman et al., 2020), where the average on-street occupancy was set to $\phi = 99.7\%$). Then, they start circling around it and possibly spiral farther and farther away from it, before eventually quitting the search or heading for an off-street parking lot, after a few minutes (Fulman et al., 2020) or more (SARECO / Prédit-Ademe, 2005; Levy et al., 2013; Weinberger et al., 2020; Fulman and Benenson, 2021). For drivers that keep searching, the time to park is believed to also depend on the turnover rate of parked vehicles (SARECO / Prédit-Ademe, 2005) and the competition with other cruising cars (SARECO / Prédit-Ademe, 2005; Arnott and Williams, 2017).

*2.2. Real search times elude common approaches*

Despite the interdependence of the search time $T_s$ and parking choices, it is tempting to try and assess the former on the basis of simple considerations. To this end, and throughout the paper, let us consider a situation in which the parking supply and the global volume of parking demand are constant. Supposing that the average occupancy $\phi$ of parking spots is known, a basic but nonetheless very common approximation (Anderson and De Palma, 2004; Geroliminis, 2015) assumes that cars move along lanes of spots that are randomly occupied with uniform probability $\phi$, and park in the first available space that they encounter. This is the theoretical foundation of the *binomial approximation* $T_s \simeq \frac{T_0}{1-\phi}$, where $T_0$ is the time to drive from one spot to the next one. According to this formula, for $\phi \leqslant 99\%$, the mean search time cannot be significantly longer than $100\,T_0$, which is around one minute if spots are adjacent. This result is manifestly at odds with the empirical observation of surging search times long before $\phi$ reaches 100% (Arnott and Williams, 2017; Gu et al., 2020; Weinberger et al., 2020); in San Francisco, Weinberger et al. (2020) even suggest the blocks where cruising cars eventually park might be occupied only at $\phi = 59\%$. In any event, the time to park is drastically underestimated by this approximation and *ad hoc* corrections to mitigate the discrepancy issue (Belloche, 2015) are devoid of theoretical ground.

Arnott and Williams (2017) rationalised this underestimation by the following factors:

1. there are spatial correlations between occupied spots [2],
2. the occupancy is not constant in time, but undergoes statistical fluctuations, and periods of higher occupancy have a stronger impact on the mean search time,
3. the competition between searching cars aggravates the difficulty of the search,
4. circling leads to inefficient double checks.

A simple model with cars moving along a circle strewn with 100 spots and parking in the first available spot was simulated to illustrate these effects, yielding search times 44% larger than the binomial estimate at an occupancy $\phi \leqslant 67\%$; unfortunately, the authors could not explain this effect from an analytical standpoint. More broadly speaking, it is critical to realise that (regardless of the selection bias in scientific works on the topic that favours situations with more acute parking issues) the parking occupancy $\phi$ is a spatio-temporal aggregate, obtained by averaging observations over a geographic area and sampling them in, or averaging them over, a time period. Since the relation between occupancy and search time is non-linear, this averaging procedure washes away the oversized impact of long cruising times near hot spots at rush hours.

On the other hand, Weinberger et al. (2020) insist on the role of the drivers' idiosyncratic behaviours in generating excess travel distances (perhaps they have kept driving because they were arguing about where to go for dinner or trying to lull a baby to sleep); the excess travel may be misapprehended for cruising (e.g., using GPS data) in districts of San Francisco and Ann Arbor where there is actually no lack of vacant spots. For the specific case of San

[2] This 'bunching' effect was later addressed analytically by Krapivsky and Redner (2019, 2020) and an approximate expression was proposed by Fulman and Benenson (2021) if the per-block occupancy is known

Francisco, Millard-Ball et al. (2020) further note that cruising is actually rare because the lack of vacant spots may be internalised in the regular drivers' behaviours and 'perceived parking scarcity leads drivers to stop short of their destinations', thus curtailing cruising. However, these caveats do not suppress the ample evidence of cruising for parking in other cities (SARECO / Prédit-Ademe, 2005; Shoup, 2006; Hampshire and Shoup, 2018; Cookson and Pishue, 2017).

To settle the debate about the actual parking pain, it is essential to gain insight into what governs the parking search time and its dependence on the occupancy in realistic settings. The following sections will blaze a theoretical trail to do so in a rigorous and generic way. But let us first highlight the influence on parking search of oft-overlooked features, in particular the topology of the explored street network and the fact that parking spaces are not equally attractive to drivers. These effects will be illustrated with particularly simple, somewhat caricatural examples in this section, before delving into the technical complexity of more general settings.

### *2.3. Topology of the street network*

While previous *theoretical* endeavours have considered linear or circular geometries for parking lanes (Levy et al., 2013; Krapivsky and Redner, 2019, 2020; Arnott and Williams, 2017), in reality parking spaces are located on a geometrically more complex network of streets (or alleys in the case of a parking lot), whose topology constrains the motion of the cars. Specific street networks have been studied *numerically*, with a more or less realistic description of their characteristics (see the review in (Boujnah, 2017)), but the sensitivity of the results to the topology has not been investigated.

Nevertheless, it is easy to understand that, for an equal number of on-street spots, their distribution along the streets and the topology of the network will affect the disutility associated with parking. First consider the simple case illustrated in Fig. 1 with a single major destination point (hot spot) and no off-street parking facility. Under equal demand, parking issues will be all the more severe as they are few streets allowing parking on the curb that lead to the hot spot. With fewer incoming streets, it will be harder to find a spot close enough to the destination.

Even if drivers park in the first vacant spot that they encounter, the network topology will matter. To understand this, we turn to the two examples of parking lots displayed in Fig. 1, where cars are injected at constant rate at the entrance and spots are located at exactly the same positions in space but are not accessible in the same way: In topology (A), cars enter one of the 9 parallel branches from the main alley on the top of the sketch, with equal probabilities for each (which is done by setting the turning probabilities adequately), whereas in topology (B) cars visit the alleys sequentially, driving by every spot before returning to the entrance point. At low occupancy, the search time will be mostly constant constant in topology (A), resulting from the travel time along the main alley on the top, whereas it will increase almost linearly with the occupancy in topology (B), as the first spots get more and more occupied. These intuitions are confirmed by the numerical results (with the protocol detailed in Section 3.2) shown in Fig. 1, which evidence a crossover (around $\phi_c \approx 40\%$) from

a low-occupancy situation with shorter searches in topology (B) to the opposite case when $\phi > \phi_c$. At high occupancies ($\phi$ >80% or 90%), the mean search time starts to be dominated by the periods of time when the parking lot is full, because of statistical fluctuations, and cars have to circle several times before a parked car leaves. The search time then surges dramatically and diverges to $\infty$ as $\phi \to 100\%$, with a possibly steeper increase in topology (A), where the rare vacant spot may be found only after several loops. Obviously, the binomial approximation can explain neither the steepness of this divergence, nor the differences between topologies (A) and (B) at moderate occupancies.

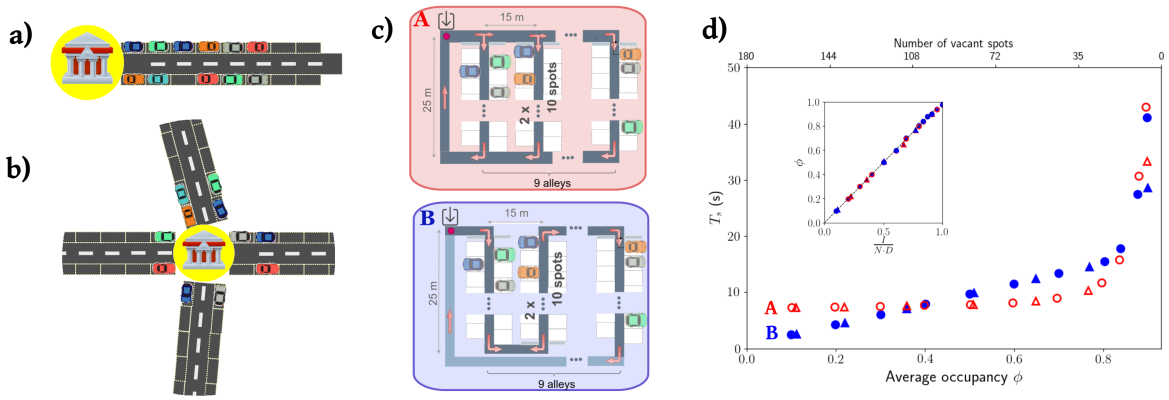


Figure 1: Influence of the topology of the street network on (**a,b**) curbside and (**c,d**) off-street parking. A major destination (hot spot) is located at the extremity of a dead-end street in sketch **(a)** and at an intersection in sketch **(b)**. Panel **(c)** displays two model off-street parking lots of $N = 180$ spaces; the evolution of the search time $T_s$ in each, for drivers parking in the first vacant spot, is shown in panel **(d)** as a function of the average occupancy $\phi$. *Inset*: Relation between $\phi$ and the product of the injection rate $I$ with the parking time $D^{-1}$ [$D^{-1} = 30$ min for the triangles (△), 60 min for the circles (◯)].

More generally, it goes without saying that these topological effects can hardly be captured by approaches that are oblivious of the street network. Yet, these considerations should not be regarded as merely abstract, as they have contributed to shaping cities and land (Shoup, 2018, intro.); this is perhaps best exemplified by the strip geometry of strip malls in North America or retail parks in Europe, which enables customers to park directly in front of the shops.

### *2.4. Attractiveness of parking spaces*

Beyond the (fixed) structure of the street network, the way in which motorists navigate through it in search of a vacant space also matters. An archetypal example of this influence is the anonymous driver observed by Hampshire et al. (2016) who routinely circles around the free parking spaces on the edge of downtown before driving to the paying spaces downtown. Somewhat similarly, some drivers may tend to circle through the very same blocks over and over again, waiting for a spot to be freed, rather than extending their search to neighbouring streets; the recurring driving through the same blocks naturally prolongs the search, compared to the exploration of new blocks. In the same vein, the driver may refrain from parking at the first vacant spot that they encounter and exhibit distinct preferences, for instance balking at

parking too far from the destination or in a paying space when there remains a possibility to park for free (Weinberger et al., 2020).

Quantitatively, we choose to gauge the driver's willingness to park at a given spot $i$ by the probability $p_i$ that she will park there *if* she drives by this spot while it is vacant. The distribution of $p_i$ in a neighbourhood clearly affects parking search. For instance, consider the 'toy' network corresponding to a small neighbourhood of Lyon shown in Fig. 2(a); for the same demand, search times will drastically differ between a situation with equally attractive spaces ($p_i = 100\%$ for every spot $i$) and a situation in which drivers exhibit a marked preference for two lanes of attractive (e.g., free) spots at $p_i = 100\%$ and balk at parking in other (costly) spots, where $p_i = 1\%$. In the latter case, drivers are prone to circling before finding a vacant free spot and search times sky-rocket even though the network-averaged occupancy remains moderate (as also supported by the numerical simulations displayed in Fig. 2(c)).

This simple example shows how using spatially averaged occupancies to estimate parking difficulties goes completely amiss whenever there is a contrast in spot attractiveness, in which case the high occupancy of attractive spots may be balanced by their vacant counterparts. Fulman and Benenson (2021) recently improved the binomial approximation by taking into account the occupancies averaged over small neighbourhoods instead of the global one and demonstrated that it much better reproduces search times in the presence of bunching (an inherent consequence of the sequential parking process) and a spatially heterogeneous demand. Nevertheless, their approach requires simulations to estimate of the distribution of local occupancies and does not explicitly handle spots of unequal attractiveness.

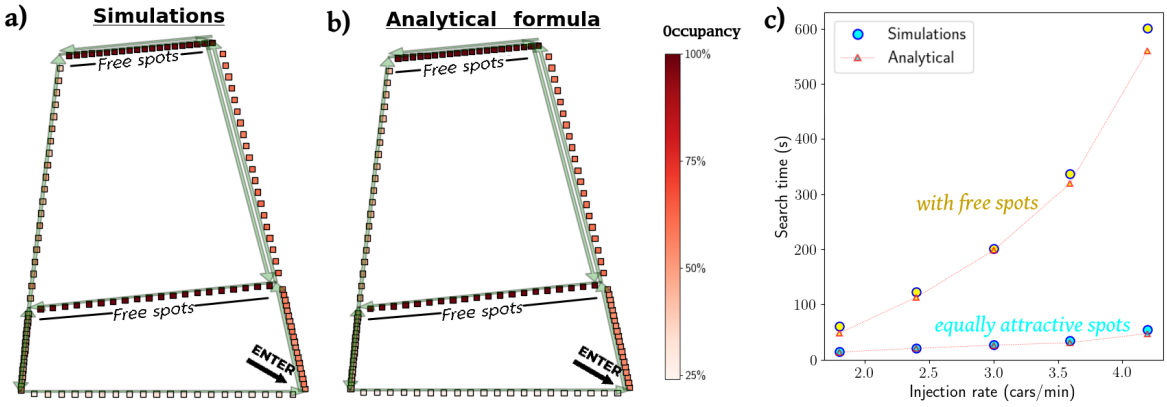


Figure 2: Influence of the inhomogeneous attractiveness of parking spots in a small 'toy' network. Cars have equal turning probabilities at each intersection. Numerically (**a**) and analytically (**b**) derived average occupancy of parking spaces (represented as squares) in the steady state, when drivers are most attracted to free spots ($p_i = 100\%$) and only have a $p_i = 1\%$ probability to park at every other vacant spot that they drive by. Panel (**c**) compares the resulting mean search times with the situation in which all spots are equally attractive ($p_i = 100\%$).

## 3. Modelling framework

To take into account the various factors discussed in the previous section, we introduce a new modelling framework, which rests on an agent-based model with high spatial resolution. Unlike its forebears, this framework does not postulate specific behavioural rules for the drivers looking for parking. Its generic formulation opens the door to a theoretical resolution through the recourse to graph theoretical and statistical physical methods. Besides, it will allow a very efficient numerical implementation.

The model relies on an explicitly described network of streets (or parking alleys), with parking spots located along them. Car drivers are grouped into distinct categories $\alpha = 1, 2, \ldots$ depending on their destination, trip purpose, etc. At an intersection (which is a node of the graph representing the network), they turn into an outgoing street with a probability given by the corresponding entry of the category-dependent turn-choice matrix $\underline{\underline{T}}^{(\alpha)}$. Finally, when driving by a spot $i$, they will choose to park there with probability $p_i^{(\alpha)}$ if it is vacant. Parked cars leave their space, and are thus removed from the simulation, at a rate $D^{(\alpha)}$, which is the reciprocal of the average parking duration.

Now, in principle, the on-site parking probability $p_i^{(\alpha)}$ depends on a variety of explanatory variables, first of which the parking rate, the distance to destination, and the odds of finding a 'better' spot estimated by the driver (Levy et al., 2013; Bonsall and Palmer, 2004), viz.,

$$p_i^{(\alpha)} = f(\text{rate}, \text{distance}, ...). \tag{1}$$

A central idea of the model is to subsume all these variables into two generic variables: (i) an attractiveness $A_i^{(\alpha)}$ reflecting how attractive a spot $i$ is perceived to be *intrinsically*, (ii) the driver's perception of how easy it currently is to park, $\beta^{(\alpha)} \in [0, \infty)$.

$$p_i^{(\alpha)}(t) = f(A_i^{(\alpha)}, \beta^{(\alpha)}(t)). \tag{2}$$

At very low occupancy, when parking seems extremely easy, viz., $\beta \to \infty$, the driver will refuse to park anywhere but in their preferred spot, of attractiveness $A_{\max}$. To the opposite, at extremely high occupancy, $\beta$ will tend to zero and virtually any admissible spot (of perceived attractiveness $A_i^{(\alpha)} > -\infty$) will be deemed acceptable, viz. $p_i^{(\alpha)} = 1$. Since $p_i^{(\alpha)} \in [0, 1]$, these considerations invite us to express $p_i$ using a Boltzmann-like functional form, viz.,

$$p_i^{(\alpha)}(t) = e^{\beta^{(\alpha)}(t) \cdot (A_i^{(\alpha)} - A_{\max})}. \tag{3}$$

At this stage, we should stress that, in practice, much will depend on the behavioural choices implicitly encoded in the attractiveness field $A_i^{(\alpha)}$ and the route choices governed by $\underline{\underline{T}}^{(\alpha)}$. Our reasoning holds for any such choices, whether they are realistic (as we claim for those made in Section 4) or not. Therefore, it reaches far beyond current studies focusing on specific rules. In this regard, note that our general formulation encompasses these rules, whether they prescribe to park in the first vacant spot within a radius of the destination (Fulman and Benenson, 2021) (which we interpret as $\beta^{(\alpha)} \simeq 0$ and $A_i$ equal to $-\infty$ outside the admissible

radius and 0 inside) or they assess the odds of finding a vacant spot before the destination (Benenson et al., 2008) (which is similar, at high occupancy, to setting $\beta^{(\alpha)} = 1 - \phi$ and $A_i$ as the negative of the distance from spot $i$ to the destination, measured in number of spots).

### *3.1. Simplifications for the current study*

Despite our wish to develop a very general model for parking, we will make a number of simplifications in this ground-laying work.

First, while in principle each driver evaluates their own $\beta$ depending on their experience along their trajectory, here we assume that $\beta^{(\alpha)}(t)$ only depends on the currently occupied spots in the network. For our practical tests, we will even assume that this parameter is a function of the global occupancy $\phi(t)$, $\beta^{(\alpha)}(t) = f[\phi(t)] \equiv \beta$.

Secondly, each category of drivers will keep a constant strategy during their search. In other words, while in reality drivers may modify their turn choices and their perception of spot attractivenesses $A_i^{(\alpha)}$ over time, for instance if they see that their preferred spot is occupied, here the turning probabilities and attractivenesses will be prescribed once and for all. (Note, however, that the actual turn choices and parking decisions may vary due to stochasticity, in our probabilistic framework).

Finally, for simplicity, we do not describe the interaction between cruising cars and the rest of the traffic and thus define fixed circulation speeds for each street. It follows that there is no point in simulating cars after they have left their parking space; they will simply vanish. Besides, we recall that a fixed initial parking demand is considered here; the feedback of parking search times on the parking demand is left outside the scope of this study.

### *3.2. Numerical implementation*

The model is implemented in C++ using data structures that lead to optimal computational performances. The nodes (i.e., intersections) and edges (i.e., street portions) of the network, and if needed the locations and attractivenesses of spots, are read from CSV files as input and used to create objects of the Spot, Node, Street, and City classes. At each time step ($dt = 1\,\mathrm{s}$ in general), a number of car objects set by a Poisson process of parameter $I$ (where $I$ is the global injection rate) are instantiated and injected into the network at one of the entry points. Their positions are measured relative to their current street and are updated iteratively at each time step. They switch streets upon reaching one intersection by randomly selecting an outgoing street according to the specified turning probabilities. We keep track of the (time-ordered) list of spots by which they have driven during the current time step and loop over it to test whether they have chosen to park at any of them, depending on the attractiveness of the spot and the (constantly updated) parking tension parameter $\beta$. At each time step, another iteration over currently parked cars removes them with a probability set by their departure rate $D^{(\alpha)}$. (The numerical results shown in the previous section were obtained with this implementation.)

Let us finally underline that in our implementation each street is linked to all incoming and outgoing streets and has access to the list of spots located along it; this allows optimal computational efficiency.

### *3.3. Mean-field analytical solution for the search time*

Once thus posed, the problem is amenable to theoretical handling. Indeed, having abstracted human behaviour and strategies, we are left with the physical problem of self-propelled particles (namely, cars) moving on a directed graph (the street network) and having known probabilities to adsorb at any site (parking spot) along the edges (streets) of this graph.

From now on, it will be more convenient to consider that every street position associated with a parking spot as well as every intersection are nodes of this graph (notice that the street position where the car starts to park and the parking spot will share the same node label). The instantaneous number of cars of category $\alpha$, $\alpha$-cars, at each node is then represented by a vector $\underline{V}^{(\alpha)}(t)$ of size $N_{\text{nodes}}$, where $N_{\text{nodes}}$ is the number of nodes and $V_i^{(\alpha)}(t) \in [0,1]$ is the number of cars at node $i$ and time $t$ averaged over random realisations. The drivers' turn choices at the nodes define a transition matrix $\underline{\underline{T}}^{(\alpha)}$ such that $T_{ij}^{(\alpha)} \in [0,1]$ is the probability that an $\alpha$-car chooses to move from node $i$ to node $j$ along an edge of the graph in one arbitrary time step, *if* it does not park in the meantime. In this graph theoretical approach, $\alpha$-cars initially injected at nodes $j$ (hence, $V_j^{(\alpha)}(t=0) > 0$) will be located at positions represented by $\underline{V}^{(\alpha)}(t=1) = \underline{V}^{(\alpha)}(0) \cdot \underline{\underline{T}}^{(\alpha)}$ at the next time step and at

$$\underline{V}^{(\alpha)}(K) = \underline{V}^{(\alpha)}(0) \cdot \left(\underline{\underline{T}}^{(\alpha)}\right)^K \tag{4}$$

after $K$ steps, *if they do not park in the mean-time*. However, at each spot $i$, cars may actually have parked, with a probability $\tilde{p}_i^{(\alpha)}$ given by $\tilde{p}_i^{(\alpha)} = p_i^{(\alpha)}\,\hat{n}_i$, where $\hat{n}_i = 1 - n_i$ is zero (one) if the spot is vacant (occupied). Taking this possibility to park into account, the transition matrix $\underline{\underline{T}}^{(\alpha)}$ should be replaced by $M_{ij}^{(\alpha)} = (1 - p_i^{(\alpha)}\,\hat{n}_i) \cdot T_{ij}^{(\alpha)}$ and the spatial distribution of cars at $t = K$ is actually

$$\underline{V}^{(\alpha)}(K) = \underline{V}^{(\alpha)}(0) \cdot \left(\underline{\underline{M}}^{(\alpha)}\right)^K. \tag{5}$$

Provided that the occupancy field $(n_i)$ is known, the probability that an $\alpha$-car injected at reaches spot $j$ and parks there reads

$$\begin{aligned} P_j^{(\alpha)} &= \sum_{K=0}^{\infty} V_j^{(\alpha)}(K) \cdot \tilde{p}_j^{(\alpha)} \\ &= \underline{V}^{(\alpha)}(0) \cdot \sum_{K=0}^{\infty} \left(\underline{\underline{M}}^{(\alpha)}\right)^K \cdot \tilde{p}_j^{(\alpha)} \\ &= \underbrace{V_i^{(\alpha)}(0)\left[\left(\underline{\underline{\mathbb{I}}} - \underline{\underline{M}}^{(\alpha)}\right)^{-1}\right]_{ij}}_{R_j^{(\alpha)}} \tilde{p}_j^{(\alpha)}, \end{aligned} \tag{6}$$

where Einstein's summation convention (on repeated indices, excluding fixed index $j$ here) is implied and $\underline{\underline{\mathbb{I}}}$ is the identity matrix. Here, we have considered that the occupancy field $(n_i)$ remains unchanged during the search, which will not hold true in the regime of strong competition between cruising cars.

Along the same lines, the average 'driving, searching, and parking' time $\mathrm{T}_s^{(\alpha,j)}$ of an $\alpha$-car finally parking at spot $j$ (in arbitrary time steps) can be derived; it is the average number of steps $K$ needed to park at spot $j$, weighted by the probability $V_j(K)\cdot\tilde{p}_j^{(\alpha)}$ to reach $j$ after $K$ steps and park there. Accordingly, summing over all spots $j$,

$$\begin{aligned}
\mathrm{T}_s^{(\alpha)} &= \sum_{K=0}^{\infty} K\; V_i^{(\alpha)}(0)\cdot\Big[\underline{\underline{M}}^{(\alpha)\,K}\Big]_{ij}\cdot\tilde{p}_j^{(\alpha)} \\
&= V_i^{(\alpha)}(0)\sum_{K=0}^{\infty}\sum_{l=0}^{K-1}\cdot\Big[\underline{\underline{M}}^{(\alpha)\,K}\Big]_{ij}\cdot\tilde{p}_j^{(\alpha)} \\
&= V_i^{(\alpha)}(0)\cdot\sum_{l=0}^{\infty}\Big[\sum_{K=l+1}^{\infty}\underline{\underline{M}}^{(\alpha)\,K}\Big]_{ij}\cdot\tilde{p}_j^{(\alpha)} \\
&= V_i^{(\alpha)}(0)\cdot\sum_{l=0}^{\infty}\Big[\underline{\underline{M}}^{(\alpha)\,l+1}\cdot\Big(\underline{\underline{\mathbb{I}}}-\underline{\underline{M}}^{(\alpha)}\Big)^{-1}\Big]_{ij}\cdot\tilde{p}_j^{(\alpha)} \\
&= V_i^{(\alpha)}(0)\cdot\Big[\underline{\underline{M}}^{(\alpha)}\cdot\Big(\underline{\underline{\mathbb{I}}}-\underline{\underline{M}}^{(\alpha)}\Big)^{-2}\Big]_{ij}\cdot\tilde{p}_j^{(\alpha)}. \qquad (7)
\end{aligned}$$

Equations 6 and 7 involve matrices of linear dimension $N_{\mathrm{nodes}}$, which may be very large. However, since each node is connected to a few other nodes at most, these matrices (notably $\underline{\underline{M}}^{(\alpha)}$) are particularly sparse. Therefore, their multiplication and inversion can be handled quite efficiently, for instance using the dedicated Python library; in particular, we avoid computing the inverse of sparse matrix $\underline{\underline{A}}\equiv\underline{\underline{\mathbb{I}}}-\underline{\underline{M}}^{(\alpha)}$ and, instead calculate $\underline{Y}\cdot\underline{\underline{A}}^{-1}$ by solving the linear problem $\underline{X}\cdot\underline{\underline{A}}=\underline{Y}$.

Incidentally, should an upper bound $K_{\max}$ be set on the number of steps $K$ allowed for parking search before cars quit searching, the foregoing expressions will turn into (see Appendix A.2 for the details)

$$\bar{P}_j^{(\alpha)} = P_j^{(\alpha)} - V_i^{(\alpha)}(0)\Big[\Big(\underline{\underline{\mathbb{I}}}-\underline{\underline{M}}^{(\alpha)}\Big)^{-1}\cdot\underline{\underline{M}}^{(\alpha)\,K_{\max}+1}\Big]_{ij}\tilde{p}_j^{(\alpha)} \qquad (8)$$

$$\bar{\mathrm{T}}_s{}^{(\alpha)} = \mathrm{T}_s^{(\alpha,j)} - V_i^{(\alpha)}(0)\cdot\Big[(\underline{\underline{\mathbb{I}}}-\underline{\underline{M}}^{(\alpha)})^{-2}\cdot\underline{\underline{M}}^{(\alpha)\,K_{\max}+1}\Big]_{ij}\tilde{p}_j^{(\alpha)}, \qquad (9)$$

where one has arbitrarily defined as $K_{\max}$ the search time of cars that quit searching. Also note that this gives access to the survival function of the search time, that is to say, the fraction of cars that needed longer than $K_{\max}$ steps to park, which is $\sum_j\left(P_j^{(\alpha)}-\bar{P}_j^{(\alpha)}\right)=1-\sum_j\bar{P}_j^{(\alpha)}$.

In all the above formulae, the search time was expressed in arbitrary units, each unit corresponding to the time taken for a car to travel between two nodes. To recover real time units, we introduce an auxiliary 'generating' function $\underline{\underline{N}}(z)$ defined by $N_{ij}(z)=z^{\tau_{ij}}\,M_{ij}^{(\alpha)}$,

where $z$ is a real variable and $\tau_{ij}$ is the travel time between neighbouring nodes $i$ and $j$ (note that, if $i$ and $j$ are not directly connected, then $M_{ij} = 0$). As with the transition matrix, exponentiating $\underline{\underline{N}}(z)$ into $\underline{\underline{N}}^K(z)$ gives access to paths of length $K$ steps. This contrivance, detailed in Appendix A.1, helps us express the search time in real time units as

$$T_s^{(\alpha)} = V_i^{(\alpha)}(0) \cdot \left[ (\underline{\underline{\mathbb{I}}} - \underline{\underline{M}}^{(\alpha)})^{-1} \cdot N'(z=1) \cdot (\underline{\underline{\mathbb{I}}} - \underline{\underline{M}}^{(\alpha)})^{-1} \right]_{ij} \tilde{p}_j^{(\alpha)}, \tag{10}$$

where the derivative of $\underline{\underline{N}}(z)$ satisfies $N'_{ij}(z=1) = \tau_{ij} M_{ij}^{(\alpha)}$

The foregoing formulae were derived for a *given* configuration of the occupancy $\underline{n}$. To get the actual *mean* search time requires averaging over an ensemble of equivalent realisations of $\underline{n}$ (or over time in the steady state). This would be straightforward if one could compute the average by plainly substituting $\langle n_j \rangle \in [0,1]$ for $n_j = 0$ or 1 in the definition of the $M_{ij}$ matrix. Unfortunately, in general, spatio-temporal correlations between spot occupations $n_i$ prohibit such a factorisation. Still, albeit not strictly rigorous, this is a valid approximation in the *mean-field* regime, wherein any mutual dependence between instantaneous spot occupations is neglected. We expect it to be quite reasonable as long as the search time is not dominated by cars looping over the very same street blocks over and over again, and we thus have an equation (Eq. 10) relating the drive-and-search time to the occupancy field ($n_i$) in this case. Conversely, when circling starts to prevail, the approximation will lose its accuracy.

### *3.4. Analytical solution for the occupancy in the stationary state*

Up to now, it has been assumed that the occupancy of each spot (or its time average) is known. We now purport to show that this occupancy field can be derived theoretically, at least in some regimes. This is achieved by balancing the probability to reach a spot and park there for an incoming car with the rate of departure of a car parked at this spot. Generally speaking, the resulting equations will display a dependence on the initial occupation. In this study, we restrict our attention to the stationary state, where this dependence is washed away so that methods from steady-state statistical physics are directly applicable. In other words, in the considered time period, the parking demand is assumed to evolve slowly enough to strike a balance between incoming $\alpha$-cars and departing ones, viz.,

$$0 = (1 - p_{\text{leakage}}^{(\alpha)}) I^{(\alpha)} - N \cdot \phi^{(\alpha)} \cdot D^{(\alpha)}, \tag{11}$$

where, for $\alpha$-cars, $I^{(\alpha)}$ is the total injection rate and the leakage fraction $p_{\text{leakage}}^{(\alpha)}$ vanishes if all incoming drivers eventually manage to park. Therefore, if only a negligible fraction of drivers quit searching, one arrives at

$$\phi^{(\alpha)} = \frac{1}{N} \cdot \frac{I^{(\alpha)}}{D^{(\alpha)}}, \tag{12}$$

and, should all categories of cars have similar parked times $1/D$,

$$\phi = \frac{1}{N} \cdot \frac{I}{D}, \tag{13}$$

where $I = \sum_\alpha I^{(\alpha)}$.

In addition to this global balance, the rate at which cars park *at any given spot* $j$ must be balanced by the (supposedly constant) departure rate $D$ of parked cars, viz.,

$$\sum_{\alpha} I^{(\alpha)} P_j^{(\alpha)} = D\langle n_j \rangle. \tag{14}$$

Using Eq. 6, one finally arrives at the mean-field stationary occupancy

$$\langle n_j \rangle = \frac{\sum_\alpha R_j^{(\alpha)} p_j^{(\alpha)} I^{(\alpha)}/D}{1 + \sum_\alpha R_j^{(\alpha)} p_j^{(\alpha)} I^{(\alpha)}/D}, \tag{15}$$

where $R_j^{(\alpha)}$, defined in Eq. 6, implicitly depends on the $\langle n_i \rangle$'s.

Note in passing that, if there is a single category of drivers, one can express $p_j$ from Eq. 15 and, on the basis of the empirically observed occupancies $\langle n_j \rangle$, infer the *empirical attractivenesses* (or more precisely $\beta A_j$) using a fixed-point method. The problem becomes more complex in the more realistic case of multiple categories of drivers and it will be addressed in our future works.

### *3.5. Numerical validation of the theory on a small street network*

The self-consistent formula, Eq. 15, giving the stationary mean-field occupancy is solved with the fixed-point method, using an empty network ($n_j = 10^{-5}$) as an initial guess and iteratively inserting it into Eq. 15 until the solution converges. Applied to the 'toy' network of Fig. 2(a), this method yields spot occupancies $n_j$ that agree very well with the numerical results, as illustrated in Fig. 2(b), with a mean error per spot that does not exceed $\sim 5\%$. Using the analytical stationary occupancy, the search time in seconds is computed with the help of Eq. 10. Figure 2(c) demonstrates the excellent agreement with the simulation results, with the possible exception of the very competitive regime at high injection rates.

### *3.6. Implications*

The theoretical framework exposed in the previous paragraphs is somewhat technical, but it has immediate practical implications. First, it is easy to understand that, in the mean-field regime, the average parking time $1/D$ only matters relative to the parking demand quantified by the injection rates $I^{(\alpha)}$; in other words, the time unit of the problem could be reset so that $D = 1$. More importantly, these rates $D$ and $I^{(\alpha)}$ do not directly affect the mean-field parking search time $T_s^{(\alpha)}$ (Eq. 10); their effect is mediated by the occupancy field $\underline{n}$ and the average occupancy $\phi$. This notably implies that the turnover rate, although widely believed to be central for the parking tension, only impacts the parking search process via its influence on the average occupancy. Put differently, as long as the fraction of time during which spots are occupied remains constant in a homogeneous period, increasing the turnover rate does not reduce the search time. Of course, in practice, limiting the parking time by rule or by cost *will* ease the parking pain, by altering the parking demand and the average occupancy – but not *per se*.

One should however bear in mind that these results are rigorous only under the mean-field hypothesis, which notably breaks down when drivers start circling significantly and competing for freshly vacated spots. This breakdown is particularly conspicuous in the high-occupancy (i.e., rightmost) part of Fig. 1(d) (where there is no longer a unique relation between the search time and the occupancy, especially for Parking Lot A).

## 4. Large-scale application of the method: On-street parking in Lyon, France

So far, we have shown that our theoretical and numerical modelling framework is applicable in small-scale street networks, but its scalability to the larger-scale networks of actual cities has not been proven yet. This section is aimed at demonstrating that our methods are quite efficient in rendering parking search in a large city. This will be illustrated with the morning peak hour (7am to 10 am) in the city of Lyon, as of 2019, which belongs to the second urban area in France, with a municipal population around 500,000 people, and features well-known difficulties to park in its centre (SARECO / Prédit-Ademe, 2005). Let us make it clear from the outset that our aim is not to provide the most accurate picture of parking in Lyon, which would require more input data than we own, but rather to put to the test our methods in a fairly realistic case study.

In particular, we resort to crude Origin-Destination matrices for Lyon-bound cars in the morning, on the basis of the number of people living and working in each district ('*arrondissement*'), corrected by a plainly empirical factor to reflect the proportion of drivers trying to park on the curb. Note that more accurate matrices based on GPS tracking are commercially available, but expensive. More precisely, 46 injection points ('sources') are chosen in, and at the boundary of, the city. For entry points inside the boundaries, the relative rates at which cars are injected at these points depend on the population of the *arrondissement*. For points located on the boundary, they depend on the estimated inflow of cars from outside the city. The latter points account for about half of the injected cars. The global injection rate will be varied in the following. Regarding the destinations, 36 points were selected (Fig. 3) and attract a fraction of the injected cars that is roughly proportional to the local number of jobs, upon aggregation over the *arrondissement*; empirical correction factors intended to reflect the availability of private and off-street parking were introduced manually. We assume no correlation between the injection point and the destination: cars are randomly bound to a destination, with the same probabilities irrespective of where it was injected. Also note that, even though our theoretical framework can include off-street parking, only drivers looking for on-street parking are considered here; parking search will therefore be described as unsuccessful if the drivers eventually opt for off-street parking or if they give up their trip altogether.

Detailed information about the locations of the $\sim$ 84,000 on-street parking spots, their rate, and their occupancy (as of 2019) as well as the street network was provided to us by the City of Lyon. Here, their attractiveness is assumed to depend exclusively on the Euclidean distance to the driver's destination and on the parking rate (either free of charge, or 1 Euro per hour or 2 Euros per hour). The hourly rate $c_h$ in Euros is converted into an equivalent additional distance to destination $d_{\text{charge}} \approx c_h \cdot 200\,\text{m}$ by balancing the cost for a dwell time of 3 hours with the cost of walking a distance $2 \cdot d_{\text{charge}}$ (from the spot to the destination and

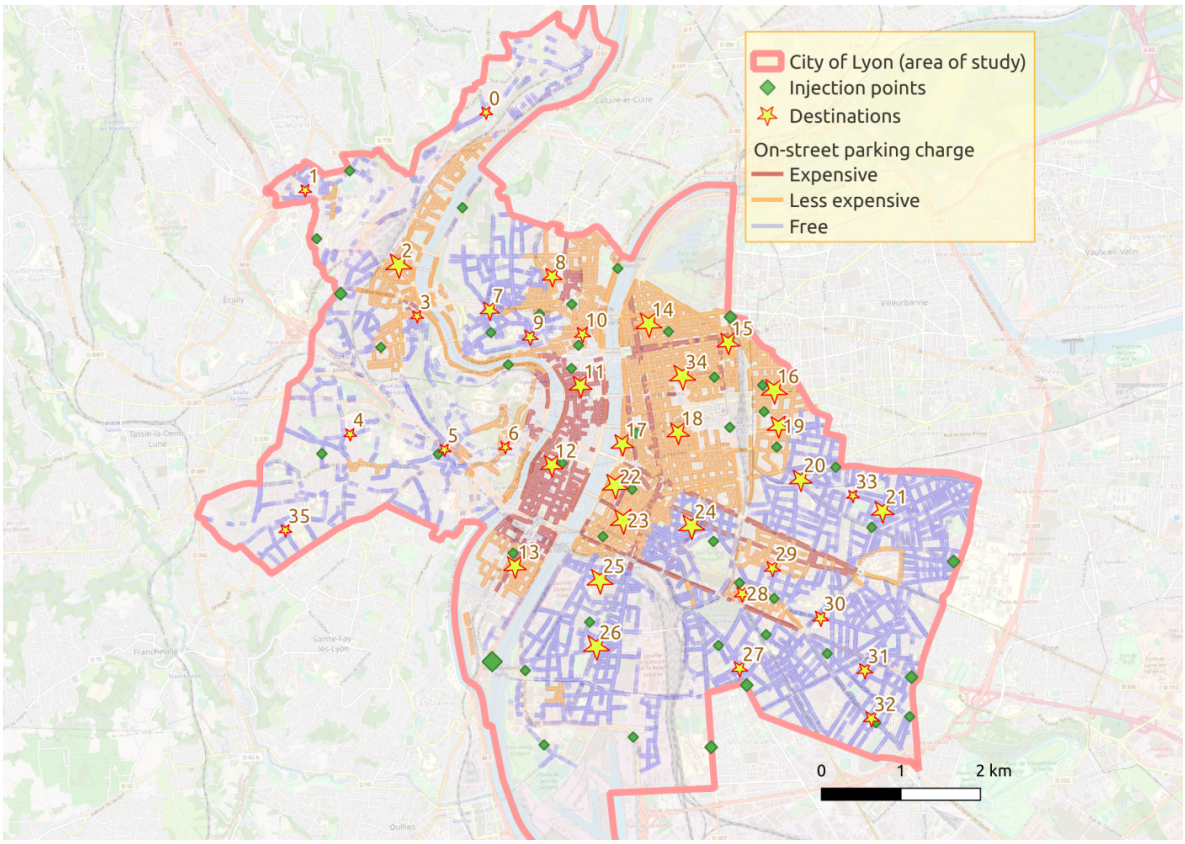


Figure 3: Map of the city of Lyon with its 84k on-street parking spots (as of 2019) and the injection points and destinations implemented in our model (the symbol sizes represent the injection rates of cars associated with these points).

the other way round), under the premise of a value of time around 13 Euros/h, multiplied by a penalty factor of 2 for the effort of walking (Bonsall and Palmer, 2004), and an effective walking speed of 1 m/s (with respect to Euclidean distances). Finally, we consider that the attractiveness decreases with the square of the distance to destination, with a characteristic length $d_{\text{walk}} = 250\,\text{m}$, so that

$$A_i = -\Big(\frac{d^{(i)}_{\text{dest}} - 200\,c_h}{d_{\text{walk}}}\Big)^2. \tag{16}$$

Regarding the perceived parking tension, we adopt the following arbitrary expression for the dependence of the tension factor on the occupancy $\phi$, $\beta = \frac{1-\phi}{2\phi^2}$, which verifies $\beta \to 0$ at very high occupancy and $\beta \gg 1$ when $\phi$ is small. In principle, $\beta$ should reflect the parking tension experienced by each user or category of users, but, for simplicity, it is here assumed to be fully correlated with the current global occupancy of the network, $\phi(t)$.

However, it should be realised that a large fraction of the existing spots will remain occupied over the whole simulation period (i.e., the morning peak hour). Estimating that 95% of spots in the centre and 87% in the periphery are occupied at a given time in the morning rush hour, this long-term occupancy was replicated by randomly declaring forbidden ('frozen') a corresponding fraction of spots, reduced by around 20% to account for cars departing during

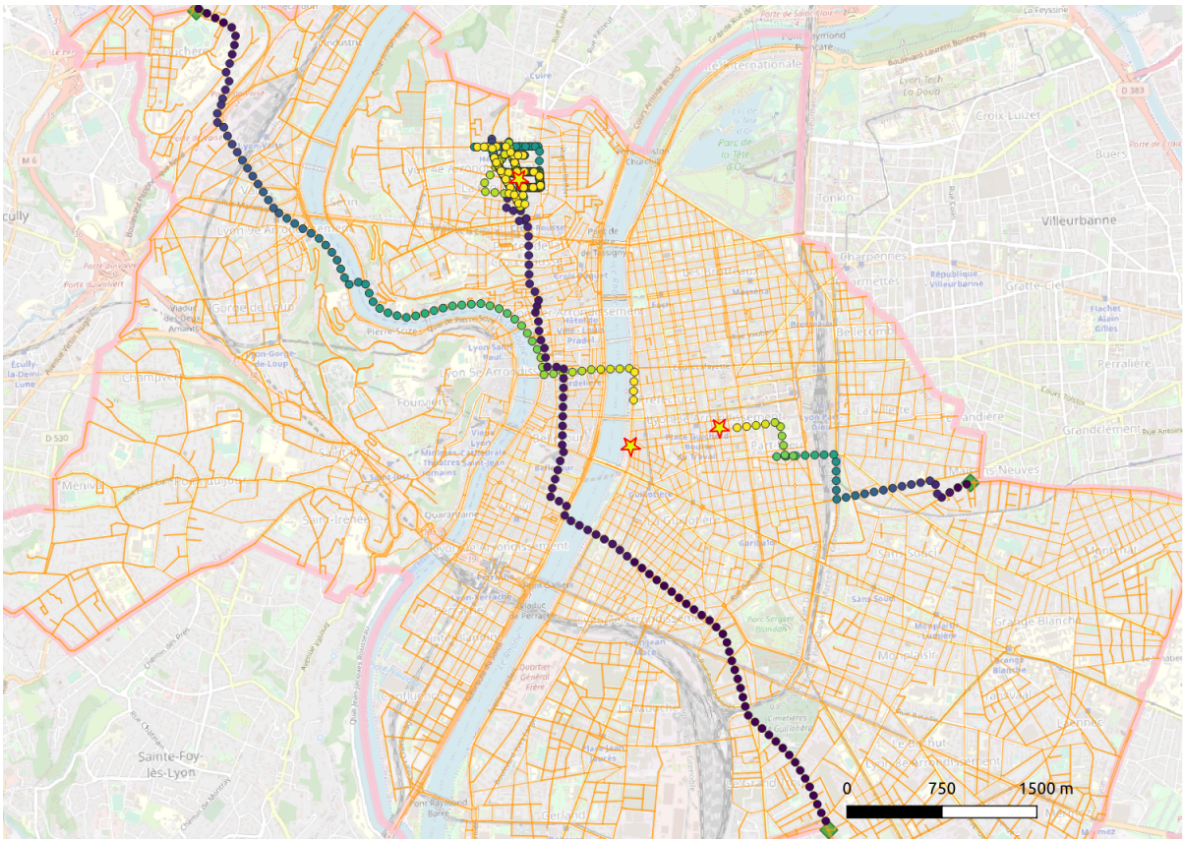


Figure 4: Examples of a few typical simulated car trajectories, from the injection point to the parking spot near the destination, represented by a star. The colours inside the circles denote the time passed since the car's entry in the network.

the simulation period. Besides, the mean parking time was set to 2.5 hours, for all destinations (note that, in any event, it cannot exceed the duration of the simulated period).

Figure 3 gives an overview of the locations and rates of parking spots, as well as the chosen injection points and destinations. Cars are directed towards their target by computing the shortest-path distance $\tilde{d}$ of every node at the end of a street portion, with the help of the Dijkstra algorithm, and favouring turns into streets whose ends are closest to the destination. Technically, for every category $\alpha$ of drivers (i.e., destination), the probability of turning into an adjacent street $\mathcal{S}_i$ when a car in street $\mathcal{S}_0$ reaches an intersection is given by

$$T_{\mathcal{S}_0 \to \mathcal{S}_i} = \frac{1}{Z} e^{\eta[\tilde{d}^{(\alpha)}(\mathcal{S}_0)] \cdot \frac{\tilde{d}^{(\alpha)}(\mathcal{S}_0) - \tilde{d}^{(\alpha)}(\mathcal{S}_i)}{l_i}}, \tag{17}$$

where $l_i$ is the length of street portion $\mathcal{S}_i$, $Z$ is a normalising factor that makes the turning probabilities to adjacent streets sum to one, and the coefficient $\eta(\tilde{d}) = \min(5, \frac{\tilde{d}}{500\,\mathrm{m}})$ results in more deterministic trajectories far away from the destination and more fluctuations when approaching it or while cruising, where circling or spiralling behaviours are expected. We do not explicitly model the interactions with transit-related traffic and assume that cars have a constant speed $v \approx 22\,\mathrm{km/h}$ throughout the city in the morning peak hour. Typical

examples of car trajectories to their parking spot, simulated with these turning probabilities, are presented in Fig. 4. One can see that the route choices to the target destination look reasonable and that they are possibly followed by circling in the vicinity of the destination if no attractive spot is found in the first place.

Our highly efficient computational methods allow us to simulate the driving and parking of $\sim 10^4$ cars in the whole city (containing $\sim 10^4$ street blocks) over a period of 3 hours in a matter of tens of seconds, using a single CPU core on a personal laptop. The outcome of the simulations in terms of average travel times (including parking search) is shown in Fig. 5, as a function of the global injection rate, and distinguished between destinations in Fig. 6.

It must be plainly admitted that we lack empirical data to gauge the accuracy of these numerical results. At best, we can say that the travel times reported in Fig. 6 are compatible with the average time spent in trips in a day, which lies around 70 minutes in the Lyon area (Sytral / Agence d'Urbanisme aire métropolitaine Lyonnaise, 2018), but this compatibility is more a safety check than a stringent validation. Furthermore, the output of the model in terms of spot occupancy cannot be used as a touchstone, because empirical occupancy data were used as model input. Regarding the excess travel times due to parking search, i.e., the difference between the observed travel times and those found for vanishing demand (injection rate), it is quite reassuring that they can reach 5 to 10 minutes at reasonable injection rates (Fig. 5), which is broadly consistent with the older data collected in (SARECO / Prédit-Ademe, 2005). Incidentally, focusing on this total driving time rather than on the search time enables us to circumvent the ambiguous definition of the start of the parking search or the onset of cruising, which was pointed out in (Millard-Ball et al., 2020). Lastly, the 'search times' are found to be strongly dependent on the destination and on the injection rate, which makes sense but also urges to take with a grain of salt empirical validations of models based on data from a single day or place. That being said, it must not be forgotten that our goal is on no account to fine-tune the calibration of the model parameters to reproduce the conditions of a specific day in Lyon as closely as possible, but instead to validate the formal connections that we have established between the occupancy and the search time, as a function of the injection rate and the drivers' preferences.

Indeed, we can now make use of the theoretical framework introduced above to get these results without resorting to extensive simulations. The parking tension factor $\beta$ is first derived from the conservation equation, Eq. 13, yielding $\phi$, and then serves as input for the fixed-point equation giving the occupancy field $n_j$, Eq. 15. This occupancy field, in turn, is used to calculate the average driving time (including parking search) via Eq. 10. Figure 5 underscores the quality of these analytical predictions in the regime of low to moderate competition for spots. The analytical results also display concordance with the numerical ones if the travel times of cars are inspected separately for every destination, as shown in Fig. 6 for an injection rate of 24 cars looking for on-street parking per minute: the root-mean-square relative error on these times is smaller than 3%, while the root-mean-square absolute error on the occupancy is under 0.04 in that case. Given the complexity of the street network, the possibly intricate car trajectories (see Fig. 4), and the multiple car categories and attractiveness fields, this agreement is remarkable. We should stress that these results were obtained using only the above analytical formulae, and not the output of the simulations; even the parking tension

parameter $\beta$ was determined theoretically.

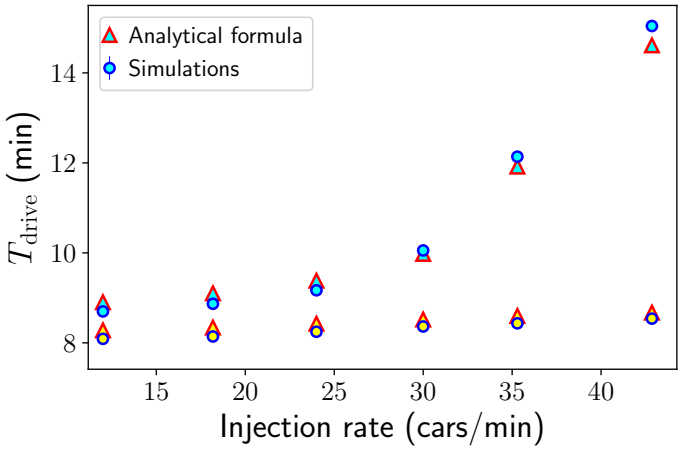


Figure 5: Dependence of the mean total driving time, including the curbside parking search time, for two categories of drivers (i.e., two destinations, irrespective of the entry point) on the global injection rate. Cyan-filled symbols represent destination 12 (Ainay), whereas yellow-filled symbols represent destination 18 (Part-Dieu).

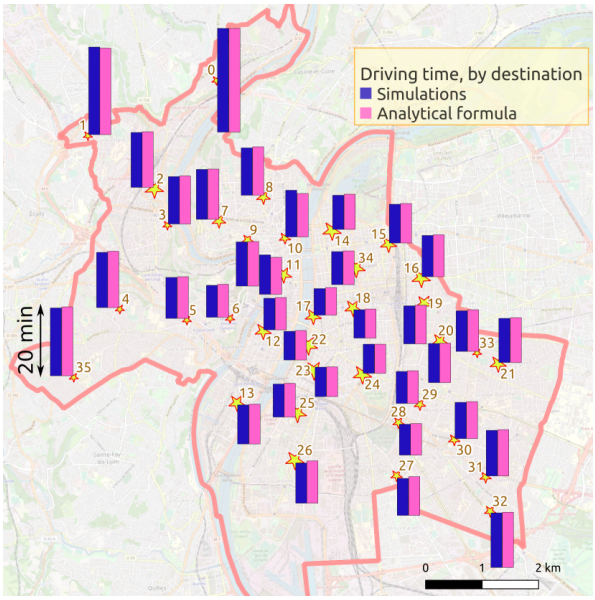


Figure 6: Map of Lyon comparing the the simulated mean total driving time and its analytically derived counterpart for all possible destinations (drivers' category), irrespective of the entry point, for a global injection rate of 24 cars/min.

## 5. Conclusions

In summary, our study of the parking search process has unveiled a quantitative relation between the total travel time and the occupancy of parking spaces, which takes into account

the effect of oft-overlooked factors such as the topology of the street network and the unequal attractiveness of parking spaces. The derived equations are quite generic and can be applied to arbitrary parking search strategies and to any street network, from simple parking lot models to large cities.

While it lays the ground for a rigorous approach to the topic, the present work involves a number of simplifications that limit its capacity to describe the reality of parking-related issues. Firstly, the framework introduced here discards possible changes in behaviour of the drivers during their search (e.g., if they have a specific favourite spot and realise that it is occupied) and it handles parking decisions spot by spot, in a sequential way, overlooking the possibility to see other spots at a distance; the drivers' perception of parking tension is also handled as a function of the occupancy of the network, instead of depending on the drivers' observations. Secondly, the generic mean-field formula that we derived for the search time requires detailed information about the occupation of spots in the network; we showed how to theoretically compute such information only in the stationary regime. Lastly, to permit the evaluation of hypothetical scenarios, the framework needs to be extended to integrate the interaction between the cruising traffic and the regular traffic and the elasticity of parking demand to search times.

Still, the parallels that have been drawn with well posed physical problems (namely, the motion on a directed graph of self-propelled particles that can adsorb on its edges) bear appealing promises: the foregoing limitations may indeed be overcome by tackling more refined physical models, which may incidentally open new avenues of research for physicists and mathematicians. Perhaps even more importantly, these abstract connections can clarify the influence of some parking characteristics on the occupancy and the search time (for instance, the parking time and the turnover rate, in this contribution).

To conclude, we would like to highlight the potential of this theoretical approach to address practically relevant issues that may be out of reach of agent-based simulations. This is particularly relevant for optimisation problems, which typically require numerous simulations that can be bypassed by our analytical formulae. We mention two such examples. First, the idea of adaptive parking pricing, whereby the attractiveness of spots is modulated by changing the parking rates, has already been experimented in San Francisco and Los Angeles, notably (Shoup, 2018). These modulations affect not only the demand, but also the parking search time (Dutta and Nicolas, 2021); our formulae relating the search time to the attractiveness in the stationary regime can help find an optimal spatial modulation of the parking rates in busy neighbourhoods. Secondly, in the context of the development of smart cities and the emergence of smart guidance and parking reservation system, our work paves the way for an assessment of the maximal performances that can be expected from smart guidance applications. This will be the focus of a forthcoming manuscript.

## Acknowledgments

We thank Y. Pachot, C. Marolleau, and N. Keller-Mayaud from the City Council services of Lyon for giving us access to empirical data about parking. This work was funded by an

Impulsion grant from IDEXLYON (2020-2021).

## Appendix A. Details pertaining to the analytical calculations

### *Appendix A.1. Search time in real time units*

In the main text, we have exposed the calculation of the search time expressed in arbitrary units (Eq. 7. In order to derive a search time in minutes, a slightly more elaborate method is needed. For that purpose, we insert the transition matrix into a 'generating' function $z \to \underline{\underline{N}}^{(\alpha)}(z)$, where $z$ is a real variable, $N_{ij}^{(\alpha)}(z) = z^{\tau_{ij}} M_{ij}^{(\alpha)}$, and $\tau_{ij}$ is the travel time from node $i$ to node $j$. At this stage, one can notice that the exponentiation of this matrix to the power $K$ yields

$$\left[\underline{\underline{N}}^{(\alpha)K}\right]_{ij}(z) = \sum_{\pi \text{ s.t. } \pi_0=0, \pi_K=j} z^{\tau_{\pi_0\pi_1}+\ldots+\tau_{\pi_{K-1}\pi_K}} \prod_{k=0}^{K-1} M_{\pi_k\pi_{k+1}}, \tag{A.1}$$

where the sum runs over permutations $\pi$ of indices (or 'paths') such that $\pi_0 = i$ and $\pi_K = j$. It immediately follows that

$$\frac{d}{dz}\left[\underline{\underline{N}}^{(\alpha)K}\right]_{ij}(z=1) = \sum_{\pi \text{ s.t. } \pi_0=0, \pi_K=j} \left(\tau_{\pi_0\pi_1} + \ldots + \tau_{\pi_{K-1}\pi_K}\right) \prod_{k=0}^{K-1} M_{\pi_k\pi_{k+1}} \tag{A.2}$$

is the probability to reach spot $j$ a number $K$ of steps after injection of the car at node $i$, multiplied by the total travel time from $i$ to $j$. The (unbound) travel time before parking thus reads

$$\begin{aligned} T_s^{(\alpha)} &= V_i^{(\alpha)}(0) \cdot \sum_{K=0}^{\infty} \frac{d}{dz}\left[\underline{\underline{N}}^{(\alpha)K}\right]_{ij}(z=1) \cdot \tilde{p}_j^{(\alpha)} \\ &= V_i^{(\alpha)}(0) \cdot \frac{d}{dz}\left[\left(\underline{\underline{\mathbb{I}}} - \underline{\underline{N}}^{(\alpha)}(z)\right)^{-1}\right]_{ij}(z=1) \cdot \tilde{p}_j^{(\alpha)} \end{aligned}$$

But, since $\frac{d\underline{\underline{A}}^{-1}}{dz} = -\underline{\underline{A}}^{-1}(z)\frac{d\underline{\underline{A}}}{dz}\underline{\underline{A}}^{-1}(z)$ for any differentiable function $z \to \underline{\underline{A}}(z)$ of invertible matrices $\underline{\underline{A}}(z)$ and $\underline{\underline{N}}^{(\alpha)}(z=1) = \underline{\underline{M}}^{(\alpha)}$,

$$T_s^{(\alpha)} = V_i^{(\alpha)}(0) \cdot \left[\left(\underline{\underline{\mathbb{I}}} - \underline{\underline{M}}^{(\alpha)}\right)^{-1} \cdot \underline{\underline{N}}^{(\alpha)\prime}(z=1) \cdot \left(\underline{\underline{\mathbb{I}}} - \underline{\underline{M}}^{(\alpha)}\right)^{-1}\right]_{ij} \cdot \tilde{p}_j^{(\alpha)}, \tag{A.3}$$

where we recall that $N_{ij}^{(\alpha)\prime}(z=1) = \tau_{ij} M_{ij}^{(\alpha)}$ and $\tilde{p}_j^{(\alpha)} = \hat{n}_j p_j^{(\alpha)}$.

Equation A.3 expresses the mean search time in minutes (or, more generally, in the same units as $\tau_{ij}$) as a function of the occupancy field $(n_j)$.

### *Appendix A.2. Capped search time in arbitrary and real time units*

Equations 6 and 7 of the main text give the mean search time of drivers that will hypothetically keep cruising forever. In reality, one expects them to quit searching after a given time.

Let us first assume that this upper time bound is given as a number $K_{\max}$ of steps from node to node. Then, capping the search simply implies restricting the sum on $K$ in Eqs 6 and 7 to $0 \leqslant K \leqslant K_{\max}$, which yields Eq. 8 for the probability $\bar{P}_j^{(\alpha)}$ to reach spot $j$ and park there. The stationary occupancy field $(n_j)$ can then be derived iteratively by inserting the capped reaching probabilities $\bar{R}_j^{(\alpha)} \equiv \bar{P}_j^{(\alpha)}/\tilde{p}_j$ into Eq. 15.

Once the occupancy field is known, one can turn to the capped search time,

$$\begin{aligned}
\bar{\mathrm{T}_s}^{(\alpha)} &= V_i^{(\alpha)}(0) \cdot \left[ \sum_{K=0}^{K_{\max}} K \, \underline{\underline{M}}^{(\alpha)K} + \sum_{K=K_{\max}+1}^{\infty} K_{\max} \, \underline{\underline{M}}^{(\alpha)K} \right]_{ij} \tilde{p}_j^{(\alpha)} \\
&= V_i^{(\alpha)}(0) \cdot \left[ \sum_{K=0}^{K_{\max}} K \, \underline{\underline{M}}^{(\alpha)K} + K_{\max} \left( \underline{\underline{\mathbb{I}}} - \underline{\underline{M}}^{(\alpha)} \right)^{-1} \cdot \underline{\underline{M}}^{(\alpha)K_{\max}+1} \right]_{ij} \tilde{p}_j^{(\alpha)} \\
&= V_i^{(\alpha)}(0) \cdot \left[ \sum_{K=0}^{K_{\max}} \sum_{l=0}^{K-1} \underline{\underline{M}}^{(\alpha)K} + K_{\max} \left( \underline{\underline{\mathbb{I}}} - \underline{\underline{M}}^{(\alpha)} \right)^{-1} \cdot \underline{\underline{M}}^{(\alpha)K_{\max}+1} \right]_{ij} \tilde{p}_j^{(\alpha)},
\end{aligned}$$

where one has arbitrarily defined as $K_{\max}$ the search time of cars that quit searching.

Using the following identity,

$$\begin{aligned}
\sum_{K=0}^{K_{\max}} \sum_{l=0}^{K-1} \underline{\underline{M}}^{(\alpha)K} &= \sum_{l=0}^{K_{\max}-1} \sum_{K=l+1}^{K_{\max}} M^K \\
&= (\underline{\underline{\mathbb{I}}} - \underline{\underline{M}}^{(\alpha)})^{-1} \sum_{l=0}^{K-1} \underline{\underline{M}}^{(\alpha)l+1} \left( \underline{\underline{\mathbb{I}}} - \underline{\underline{M}}^{(\alpha)K_{\max}-l} \right) \\
&= \underline{\underline{M}}^{(\alpha)} \cdot (\underline{\underline{\mathbb{I}}} - \underline{\underline{M}}^{(\alpha)})^{-2} \cdot (\underline{\underline{\mathbb{I}}} - \underline{\underline{M}}^{(\alpha)K_{\max}}) - K_{\max} (\underline{\underline{\mathbb{I}}} - \underline{\underline{M}}^{(\alpha)})^{-1} \cdot \underline{\underline{M}}^{(\alpha)K_{\max}+1},
\end{aligned}$$

we arrive at

$$\begin{aligned}
\bar{\mathrm{T}_s}^{(\alpha)} &= V_i^{(\alpha)}(0) \cdot \left[ \underline{\underline{M}}^{(\alpha)} \cdot (\underline{\underline{\mathbb{I}}} - \underline{\underline{M}}^{(\alpha)})^{-2} \cdot (\underline{\underline{\mathbb{I}}} - \underline{\underline{M}}^{(\alpha)K_{\max}}) \right]_{ij} \tilde{p}_j^{(\alpha)} \\
&= \mathrm{T}_s^{(\alpha)} - V_i^{(\alpha)}(0) \cdot \left[ (\underline{\underline{\mathbb{I}}} - \underline{\underline{M}}^{(\alpha)})^{-2} \cdot \underline{\underline{M}}^{(\alpha)K_{\max}+1} \right]_{ij} \tilde{p}_j^{(\alpha)}. \qquad \text{(A.4)}
\end{aligned}$$

As in the main text, Einstein's summation convention on repeated indices is implied.

To recover real time units, we calculate an average conversion factor between steps $K$ and seconds using the case of unbound searches, by equating the (unbound) search time given by Eq. 7 and that given by Eq. 10. The maximum number of steps $K_{\max}$ is then first estimated from the maximum allowed time and the capped search time $\bar{\mathrm{T}_s}^{(\alpha)}$ is eventually converted into seconds on the same basis.

Unfortunately, evaluating the capped search time via Eq. A.4 involves the computation of $\underline{\underline{M}}^{(\alpha)K_{\max}+1}$ for $K_{\max} \gg 1$, which will not necessarily be a sparse matrix even if $\underline{\underline{M}}^{(\alpha)}$ is. This

computation turns out to be numerically very demanding if the number of nodes in the graph is huge, as in the Lyon test case. However, the method is operational and quick on smaller networks. Consider for example the 'toy' network introduced in Fig. 2(a). Capping search times to 180 s reduces the simulated mean search time all the more as the injected rate is high, as expected and shown on Fig. A.7. These capped times are very well captured by the theoretical method outlined above, culminating in Eq. A.4, as can be seen on Fig. A.7.

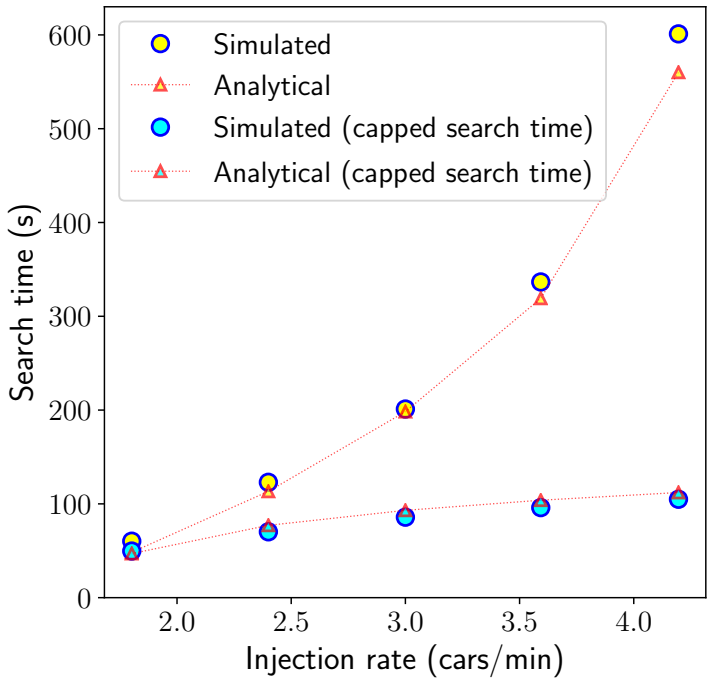


Figure A.7: Variations of the driving and cruising time in the 'toy' network of Fig. 2(a) (with free spots) with the car injection rate. The outcome of the simulation (circles) is compared with the analytical predictions (triangles), both in the case of unbound search times and when search times are capped to 180 s.

## Appendix B. Detailed input for the simulations of Lyon

Section 4 presented a large-scale application of the proposed framework in the case of the city of Lyon, France. In this application, drivers are classified into 36 categories according to their final destination (the list of which is given in Tab. B.2). Their cars are injected into the networks at one of the 49 entry points enumerated in Tab. B.4, with a relative probability inferred either from the population of the surrounding neighbourhood or on a rough estimation of the inflow from the periphery of the city, if the entry point is located at its boundary.

| Label | $x$ | $y$ | Proba of injection $V_i(0)$ |
|---|---|---|---|
| 0 | 843661 | 6520685 | 0.017 |
| 1 | 841446 | 6516539 | 0.161 |
| 2 | 844237 | 6520113 | 0.017 |
| 3 | 840046 | 6520488 | 0.024 |
| 4 | 842098 | 6515492 | 0.011 |
| 5 | 846715 | 6516345 | 0.048 |
| 6 | 846268 | 6515772 | 0.012 |
| 7 | 843023 | 6521479 | 0.017 |
| 8 | 841709 | 6517901 | 0.014 |
| 9 | 844843 | 6520013 | 0.017 |
| 10 | 846215 | 6518226 | 0.020 |
| 11 | 843218 | 6515591 | 0.011 |
| 12 | 844862 | 6519680 | 0.020 |
| 13 | 842529 | 6520514 | 0.007 |
| 14 | 844989 | 6517334 | 0.012 |
| 15 | 839541 | 6521161 | 0.064 |
| 17 | 842670 | 6517036 | 0.011 |
| 18 | 844226 | 6518050 | 0.011 |
| 20 | 841862 | 6516427 | 0.011 |
| 21 | 841071 | 6522242 | 0.017 |
| 22 | 847245 | 6517797 | 0.039 |
| 23 | 841429 | 6520673 | 0.007 |
| 24 | 844289 | 6516742 | 0.012 |
| 25 | 842837 | 6518111 | 0.011 |
| 26 | 842041 | 6520903 | 0.007 |
| 27 | 839305 | 6519151 | 0.012 |
| 28 | 839305 | 6519151 | 0.012 |
| 29 | 841647 | 6520269 | 0.012 |
| 30 | 845762 | 6518982 | 0.023 |
| 31 | 839240 | 6521852 | 0.024 |
| 32 | 846693 | 6515848 | 0.012 |
| 33 | 844198 | 6515464 | 0.048 |
| 34 | 843204 | 6518705 | 0.011 |
| 35 | 844645 | 6516244 | 0.048 |
| 36 | 840767 | 6519147 | 0.012 |
| 38 | 845656 | 6516640 | 0.012 |
| 39 | 843257 | 6519411 | 0.020 |
| 40 | 844439 | 6520869 | 0.042 |
| 41 | 844554 | 6517528 | 0.012 |
| 42 | 844889 | 6516878 | 0.012 |
| 43 | 842446 | 6521030 | 0.007 |
| 44 | 844431 | 6519483 | 0.020 |
| 45 | 845021 | 6519236 | 0.020 |
| 47 | 842325 | 6519031 | 0.015 |
| 48 | 839654 | 6522705 | 0.023 |



Table B.4: List of the 49 entry points considered for the injection of cars into the street network, with their relative probabilities. Coordinates are given in the RGF-93/Lambert-93 reference system.

## References


Al-Turjman, F., Malekloo, A., 2019. Smart parking in iot-enabled cities: A survey. Sustainable Cities and Society 49, 101608.

Anderson, S.P., De Palma, A., 2004. The economics of pricing parking. Journal of urban economics 55, 1–20.

Arnott, R., Williams, P., 2017. Cruising for parking around a circle. Transportation research part B: methodological 104, 357–375.

Axhausen, K.W., Polak, J.W., Boltze, M., Puzicha, J., 1994. Effectiveness of the parking guidance information system in frankfurt am main. Traffic engineering & control 35, 304–309.

Belloche, S., 2015. On-street parking search time modelling and validation with survey-based data. Transportation Research Procedia 6, 313–324.

Benenson, I., Martens, K., Birfir, S., 2008. Parkagent: An agent-based model of parking in the city. Computers, Environment and Urban Systems 32, 431–439.

Bonsall, P., Palmer, I., 2004. Modelling drivers' car parking behaviour using data from a travel choice simulator. Transportation Research Part C: Emerging Technologies 12, 321–347.

Boujnah, H., 2017. Modélisation et simulation du système de stationnement pour la planification de la mobilité urbaine: application au territoire de la cité Descartes. Ph.D. thesis. Paris Est.

Chatman, D.G., Manville, M., 2014. Theory versus implementation in congestion-priced parking: An evaluation of sfpark, 2011–2012. Research in Transportation Economics 44, 52–60.

Cookson, G., Pishue, B., 2017. The Impact of Parking Pain in the US, UK and Germany. Technical Report. INRIX.

Dutta, N., Nicolas, A., 2021. Searching for parking in a busy downtown district: An agent-based computational and analytical model, in: 2021 International Symposium on Computer Science and Intelligent Controls (ISCSIC), IEEE. pp. 348–354.

Fulman, N., Benenson, I., 2021. Approximation method for estimating search times for on-street parking. Transportation Science .

Fulman, N., Benenson, I., Elia, E.B., 2020. Modeling parking search behavior in the city center: A game-based approach. Transportation Research Part C: Emerging Technologies 120, 102800.

Gao, H., Yun, Q., Ran, R., Ma, J., 2021. Smartphone-based parking guidance algorithm and implementation. Journal of Intelligent Transportation Systems , 1–17.

Geroliminis, N., 2015. Cruising-for-parking in congested cities with an mfd representation. Economics of Transportation 4, 156–165.

Gu, Z., Najmi, A., Saberi, M., Liu, W., Rashidi, T.H., 2020. Macroscopic parking dynamics modeling and optimal real-time pricing considering cruising-for-parking. Transportation Research Part C: Emerging Technologies 118, 102714.

Hampshire, R.C., Jordon, D., Akinbola, O., Richardson, K., Weinberger, R., Millard-Ball, A., Karlin-Resnik, J., 2016. Analysis of parking search behavior with video from naturalistic driving. Transportation Research Record 2543, 152–158.

Hampshire, R.C., Shoup, D., 2018. What share of traffic is cruising for parking? Journal of Transport Economics and Policy (JTEP) 52, 184–201.

Krapivsky, P., Redner, S., 2019. Simple parking strategies. Journal of Statistical Mechanics: Theory and Experiment 2019, 093404.

Krapivsky, P., Redner, S., 2020. Where should you park your car? the rule. Journal of Statistical Mechanics: Theory and Experiment 2020, 073404.

Lehner, S., Peer, S., 2019. The price elasticity of parking: a meta-analysis. Transportation Research Part A: Policy and Practice 121, 177–191.

Levy, N., Martens, K., Benenson, I., 2013. Exploring cruising using agent-based and analytical models of parking. Transportmetrica A: Transport Science 9, 773–797.

Millard-Ball, A., Hampshire, R.C., Weinberger, R., 2020. Parking behaviour: The curious lack of cruising for parking in san francisco. Land Use Policy 91, 103918.

Polak, J., Axhausen, K.W., 1990. Parking search behaviour: A review of current research and future prospects. Transport Studies Units, Working Paper 540.

SARECO / Prédit-Ademe, 2005. Le temps de recherche de stationnement. Technical Report. SARECO / Prédit-Ademe.

Schadschneider, A., Chowdhury, D., Nishinari, K., 2010. Stochastic transport in complex systems: from molecules to vehicles. Elsevier.

Shoup, D., 2018. Parking and the City. Routledge.

Shoup, D.C., 2006. Cruising for parking. Transport policy 13, 479–486.

Sytral / Agence d'Urbanisme aire métropolitaine Lyonnaise, 2018. Pratiques de déplacements sur les bassins de vie du Scot de l'agglomération lyonnaise (2015). Technical Report. Sytral / Agence d'Urbanisme aire métropolitaine Lyonnaise.

Tanaka, S., Ohno, S., Nakamura, F., 2017. Analysis on drivers' parking lot choice behaviors in expressway rest area. Transportation research procedia 25, 1342–1351.

Vo, T.T.A., van der Waerden, P., Wets, G., 2016. Micro-simulation of car drivers' movements at parking lots. Procedia Engineering 142, 100–107.

Weinberger, R.R., Millard-Ball, A., Hampshire, R.C., 2020. Parking search caused congestion: Where's all the fuss? Transportation Research Part C: Emerging Technologies 120, 102781.

| Label | Name | $x$ | $y$ | Probability |
|---|---|---|---|---|
| 0 | Saint-Rambert - industrie | 841367.9 | 6523437.7 | 0.012 |
| 1 | La Duchère | 839095.5 | 6522460.5 | 0.015 |
| 2 | Vaise | 840269.9 | 6521523.7 | 0.046 |
| 3 | Champvert – Point-du-jour | 840501.8 | 6520877.9 | 0.0114 |
| 4 | Ménival - La Plaine | 839660 | 6519395.7 | 0.011 |
| 5 | Saint-Just | 840845.5 | 6519201.4 | 0.011 |
| 6 | Vieux-Lyon | 841609.7 | 6519231.4 | 0.011 |
| 7 | Chazière -Flammarion | 841413.3 | 6520955.4 | 0.028 |
| 8 | Cœur Croix-Rousse | 842199.3 | 6521377.5 | 0.028 |
| 9 | Les Chartreux | 841921.4 | 6520617 | 0.022 |
| 10 | Pentes | 842580 | 6520652.1 | 0.022 |
| 11 | Terreaux – Cordeliers | 842555.7 | 6520004.7 | 0.031 |
| 12 | Ainay | 842195 | 6519007.4 | 0.031 |
| 13 | Sud Perrache | 841731.4 | 6517736.3 | 0.031 |
| 14 | Tête d'or – Foch | 843412.4 | 6520782.8 | 0.04 |
| 15 | Brotteaux – Europe | 844411.3 | 6520546.7 | 0.032 |
| 16 | Bellecombe – Thiers | 844989.5 | 6519947.4 | 0.040 |
| 17 | Mutualité-Préfecture | 843080.8 | 6519272 | 0.032 |
| 18 | Part-Dieu - Bir Hakeim | 843782.1 | 6519416.5 | 0.032 |
| 19 | Paul Bert – Villette | 845042.8 | 6519497.8 | 0.032 |
| 20 | Dauphiné - Sans Souci | 845321.7 | 6518826.4 | 0.032 |
| 21 | Montchat | 846350.6 | 6518432.2 | 0.032 |
| 22 | Jean Macé | 842992.7 | 6518754.3 | 0.037 |
| 23 | Guillotière | 843092.8 | 6518310.3 | 0.046 |
| 24 | Blandan | 843950.4 | 6518243.7 | 0.046 |
| 25 | Gerland nord | 842799.7 | 6517560.4 | 0.046 |
| 26 | Gerland sud | 842756.2 | 6516727.5 | 0.046 |
| 27 | Grand Trou – Moulin à vent | 844554.8 | 6516452.7 | 0.02 |
| 28 | Monplaisir | 844588.2 | 6517391.2 | 0.021 |
| 29 | Le Bachut | 844966.5 | 6517711.6 | 0.021 |
| 30 | Etats-Unis | 845574.1 | 6517087.7 | 0.021 |
| 31 | Mermoz – Laennec | 846128.7 | 6516429 | 0.021 |
| 32 | Général André - Santy | 846210.7 | 6515824.3 | 0.021 |
| 33 | Pinel | 845979 | 6518623 | 0.014 |
| 34 | 6e arrondissement Sud | 843836.9 | 6520125.1 | 0.040 |
| 35 | 5e arrondissement Sud | 838846.3 | 6518189.5 | 0.011 |

Table B.2: List of the 36 destinations implemented in our study of Lyon. The 'probability' column specifies the fraction of cars bound to a given destination. Coordinates are given in the RGF-93/Lambert-93 reference system.